RESEARCH ARTICLE

Millimeter-Wave Antenna With Gain Improvement Utilizing Reflection FSS for 5G Networks

HESHAM A. MOHAMED [1], (Senior Member, IEEE), **MOHAMED EDRIES**[2],
MAHMOUD A. ABDELGHANY[3,4], (Member, IEEE),
AND AHMED A. IBRAHIM[4], (Senior Member, IEEE)

[1]Electronics Research Institute, Cairo 11843, Egypt
[2]Department of Communication and Computer Engineering, Higher Institute of Engineering, El-Shorouk Academy, El Shorouk, Cairo 11714, Egypt
[3]Electrical Engineering Department, College of Engineering, Prince Sattam Bin Abdulaziz University, Wadi Addawasir 11991, Saudi Arabia
[4]Electrical Engineering Department, Faculty of Engineering, Minia University, Minya 61519, Egypt

Corresponding author: Ahmed A. Ibrahim (ahmedabdel_monem@mu.edu.eg)

ABSTRACT A millimeter-wave (mm-wave) antenna with enhanced gain for new 5G networks is introduced in this work. A rectangular slot antenna operating at the fundamental mode of the desired frequency band is utilized in this study. The antenna gain is improved by employing a Frequency Selective Surface (FSS). The FSS-based reflectors are designed at the same fundamental mode of the antenna and added under the antenna at a specific distance to achieve the required gain enhancement with a suitable dimension of $25 \times 25 \times 5$ mm^3. The antenna gain is increased by around 5.3 dBi when the FSS-based reflectors are added under the antenna. The antenna and the FSS are fabricated and tested. The antenna has tested outcomes without FSS with $S_{11} \leq -10$ dB from 26 GHz up to 29.8 GHz and realized gain of around 4.5 dBi within the entire frequency band and radiation efficiency of around 93 %. While the antenna with FSS has achieved bandwidth with $S_{11} \leq -10$ dB from 25.5 GHz up to 30.8 GHz and realized gain around 10.3 dBi at 28 GHz and radiation efficiency around 90 %. The simulated and tested outcomes have the same trend which validates the suggested antenna to be operated in the new 5G applications. All simulation results are completed using the CST Microwave Studio.

INDEX TERMS Antenna, FSS, mm-wave, gain enhancement, 5G networks, 28 GHz.

I. INTRODUCTION

The new revolution in the mobile industry is the growth of mobile communication technologies [1]. The advancement of mobile technology generations is driven by the requirements for higher bandwidth, higher data rates, a large number of users, and reliable connectivity [2]. The fifth generation (5G) is a new technology that was developed to keep up with the increasing data rates and bandwidth [3], [4]. According to research and studies, two popular frequency bands have been allocated for 5G technologies. The lower band (i.e., sub 6 GHz) and upper band (i.e., mm waves) are the two frequency bands. The existing available sub 6 GHz band (3 – 6 GHz) is already crowded with applications, so actual communication for mm-wave with unlicensed and unrestricted bandwidth must be established [5]–[9]. In the mm-wave, bands such as 28 GHz and 38 GHz have been allocated as possible choices for future 5G standards [10]–[14]. Higher data rates and bandwidth can be achieved by using a higher portion of the spectrum. However, these frequencies are affected by atmospheric attenuation, such as rain, fog, and snow. These challenges with atmospheric attenuation can be overcome by using antennas with high gain and directivity.

There are several techniques are used to increase the gain and directivity of an antenna such as using an antenna array [15]–[18], adding an artificial magnetic conductor (AMC) below the antenna [19]–[22], and using the FSS. These techniques can be used to improve the antenna gain in

The associate editor coordinating the review of this manuscript and approving it for publication was Shah Nawaz Burokur [ID].

microwave and mm-wave [23]–[27]. In [15], a 28 GHz four elements antenna array with hocked shape is investigated to increase the single antenna gain from 3.59 dBi to 10.3 dBi. A 28 GHz five elements slot antenna array to produce antenna gain of around 10 dBi is discussed in [16]. In [17], a 28 GHz four elements dense dielectric patch antenna array attached with a superstrate to achieve antenna gain of 12.4 dBi is studied. A 26 GHz to 38 GHz eight elements antenna array is used to produce antenna gain around 10.5 dBi at 28 GHz is discussed in [18]. Also, the antenna gain can be enhanced by adding an artificial magnetic conductor (AMC) below the antenna [19]–[22]. In [19], a 33 GHz bowtie slotted antenna with AMC is introduced presented to achieve an antenna gain of 5.5 dBi. A 28 GHz patch MIMO antenna with AMC is investigated in [20] to achieve an antenna gain of 10 dBi. A 28 GHz with 7.4 dBi gain of the AMC-based patch antenna is discussed in [21]. While a 30 GHz simple patch antenna with AMC cells and gain of 9 dBi is studied in [22]. As well as the FSS can be used to improve the antenna gain in microwave and mm-wave [23]–[27]. In [25], a 28 GHz dense dielectric patch antenna attached with FSS to achieve an antenna gain of 17.5 dBi is investigated. A 28 GHz beam-tilting antenna combined with an FSS to achieve an antenna gain of 11 dBi is discussed.

In this work, a 28 GHz slot antenna attached with FSS-based reflectors to improve the antenna gain is suggested. The suggested antenna is designed to be utilized for new 5G applications. The antenna gain is increased by around 6 dBi when the FSS-based reflectors are added under the antenna. The antenna and the FSS are fabricated tested and achieved good matching between the simulated and tested outcomes. The antenna with FSS has achieved bandwidth with $S_{11} \leq -10$ dB from 25.5 GHz up to 30.8 GHz and realized gain around 10.3 dB at 28 GHz and radiation efficiency around 90%. Finally, the suggested antenna shows a small size with suitable gain and simplicity in the feeding network. The paper is divided into several sections. The introduction and the overview of 5G antenna enhancement techniques are presented in section 1. Section 2 explains the slot antenna structure design. Section 3 discusses the FSS unit cell structure design. The simulation results of the proposed slot antenna with FSS and its discussion are explained in section 4. Finally, the conclusion is written in section 5.

II. SLOT ANTENNA

The 2D configuration top and back views of the slot antenna are illustrated in Fig. 1. The 50 Ω microstrip line is placed on 4003 Rogers substrate with 3.35, 0.203 mm dielectric constant and thickness respectively. A rectangular slot is etched from a ground plane on the other side of the substrate. The antenna has a size of 12 mm × 12 mm. The antenna is ended with a launcher connector in the simulation to mimic the measurement process as shown in Fig. 1. The CST microwave studio Software is employed in the design and simulation
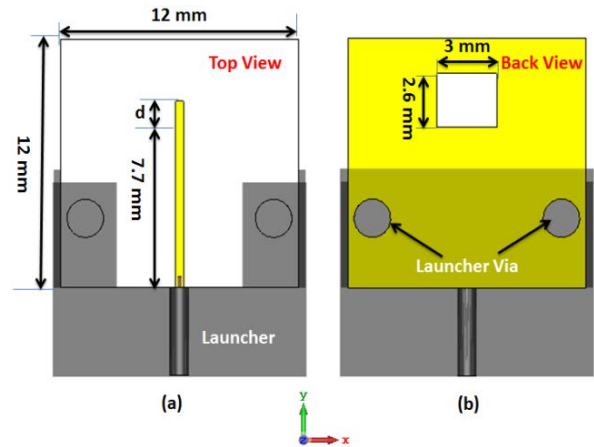

FIGURE 1. Configuration of the slotted antenna with launcher (a) Top (b) back.
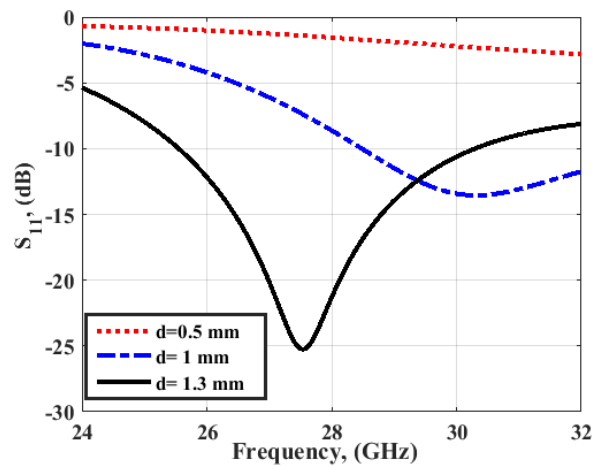

FIGURE 2. S_{11} outcomes of the slot antenna with varying microstrip length (d).

process. The microstrip line length (d) plays an important role to achieve a good matching result as shown in Fig. 2. The field is concentrated around the end of the microstrip line toward the slot and any length variation of it can affect the capacitance and inductance values which in turn affect the matching features of the slot antenna. As displayed in Fig. 2, when the microstrip length (d) is changed from 0.5 mm to 1.3 mm the antenna matching is strongly affected. When the d = 0.5 mm (the dotted red line) there is no matching inside the frequency of interest. Also, the frequency band from 28.2 GHz up to 32 GHz with $S_{11} \leq -10$ dB and a matching level around −13 dB is accomplished when d = 1 mm (the dotted dashed blue line). The matching level lower than −25 dB is achieved when the d =1.3 mm (the solid black line) with a frequency band from 25.8 GHz to 30 GHz.

The slot length and width affect the fundamental mode of the operation at 28 GHz. For more confirmation, the current distribution at 28 GHz of the slot antenna is simulated and displayed in Fig. 3. It is seen that the current is concentrated around the slot which ensures the radiation of the antenna at its fundamental mode.
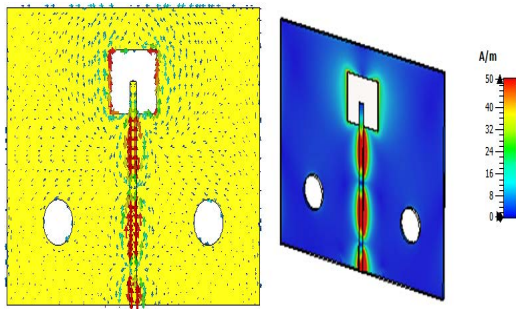
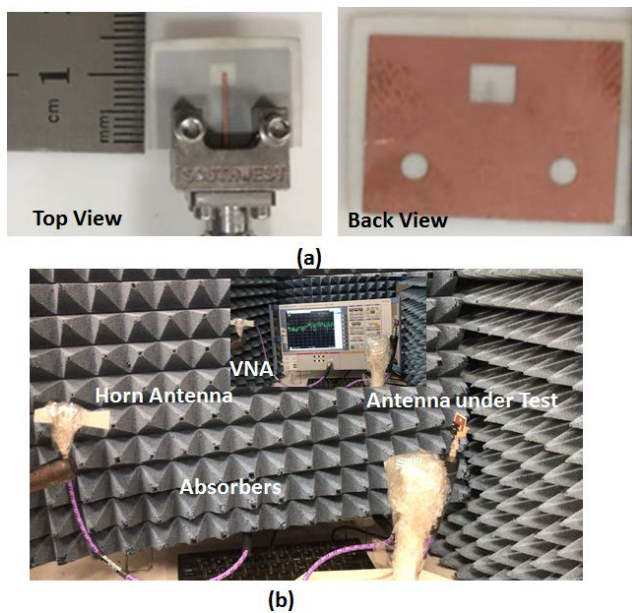**FIGURE 3.** Current distribution of the slot antenna at 28 GHz.

FIGURE 4. Slot antenna fabricated prototype (a)Top and back views (b) The radiation patterns and gain measuring setup.

FIGURE 5. S_{11} simulated and measured outcomes of the slot antenna.
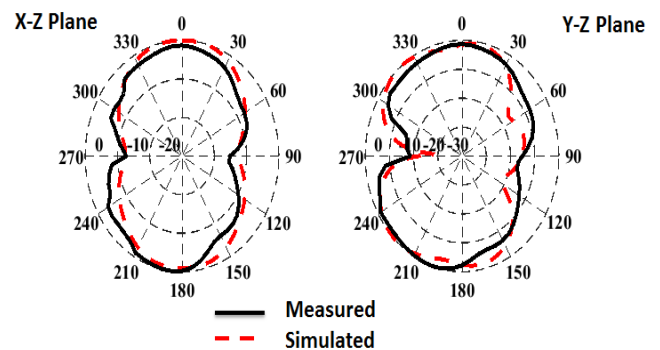
FIGURE 6. Radiation patterns (normalized) of the slot antenna at 28 GHz.

FIGURE 7. Slot antenna realized gain.

Fig. 4 (a) illustrates the fabricated top and back photos of the slot antenna prototype. The 2.4 mm launcher connector is used the utilizing in the measurement process. The antenna is connected via the launcher to the VNA Rohde & Schwarz ZVA 67 to deliver the tested reflection coefficient results as shown in Fig. 5. As shown in Fig. 5, the antenna has a simulated frequency band beginning from 25.8 GHz to 30 GHz (4.2 GHz bandwidth) with $S_{11} \leq -10$ dB. Whilst, the tested outcomes have achieved frequency band from 26 GHz to 29.8 GHz (3.8 GHz bandwidth) with $S_{11} \leq -10$ dB. As well, the simulated and measured outcomes have good consistency between them.

The anechoic chamber is used in the measuring setup as shown in Fig. 4 (b). The reference horn antenna worked from 26 GHz up to 40 GHz is used as the transmitting end while the slot antenna is added at receiving end with 65 cm space between them to achieve the far-field criteria. The line of sight direction is achieved between the two antennas. The slot antenna under test is rotated in both the horizontal and elevation planes. By linking the reference horn antenna
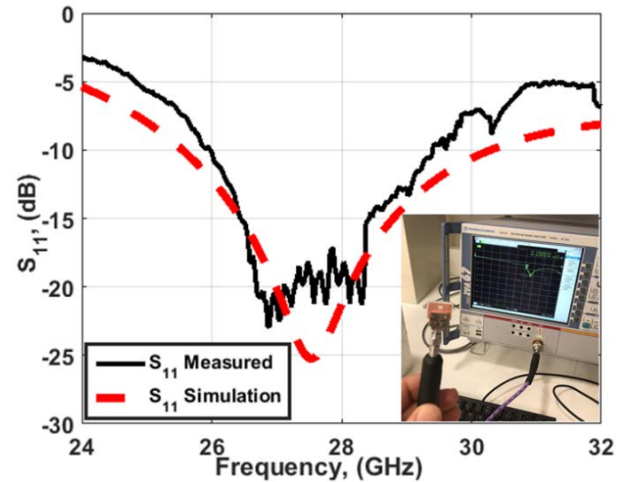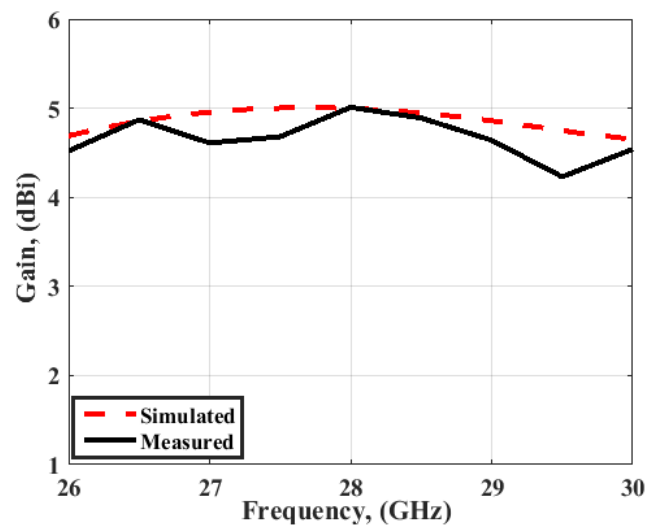
to port 2 of the Rohde & Schwarz ZVA 67 VNA and the suggested MIMO to port 1 then the gain is extracted from the tested S_{21} [28]. Fig. 6 shows the normalized simulated and tested radiation patterns outcomes at 28 GHz in the X-Z
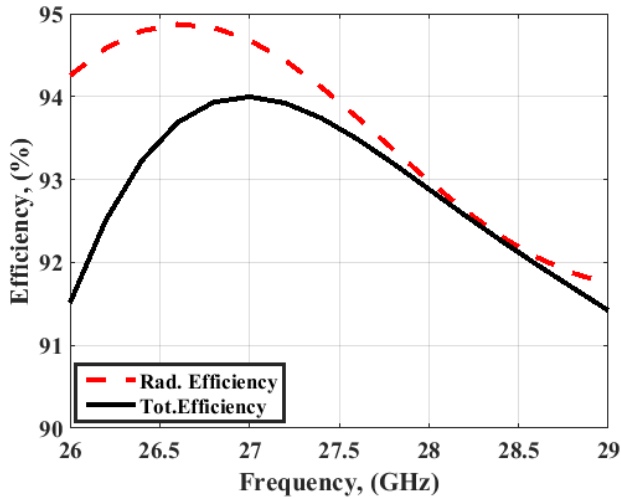
FIGURE 8. Slot antenna efficiency.

FIGURE 9. Proposed structure FSS (a) configuration of the cell (X = 5 mm, R1 = 1.8 mm, R2 = 1.6 mm, R3 = 0.5 mm, L = 1.1 mm) (b) The applied boundary conditions.

and Y-Z planes. The antenna has bidirectional patterns in both planes with a good trend between the two outcomes. Depending on the technique used in [28] and [29], the realized gain of the antenna is measured and displayed in Fig. 7. The simulated realized equals around 5 dBi within the frequency band and around 4.5 dBi is achieved from the tested results. Fig. 8 illustrated the total and radiation efficiency of the antenna. The efficiency of the antenna equals around 93 %.

III. FSS UNIT CELL STRUCTURE DESIGN

To enhance the antenna gain, The FSS-based reflectors can be employed. There are two ways to introduce the FSS with antenna structure. First, The FSS is added above the antenna and it is called transmission-based FSS and the other is added below the antenna structure and is called reflection-based antenna. In this work, we used the second technique to enhance the antenna gain by ensuring the reduction in the antenna back radiation. Fig. 9 (a) displays the suggested FSS single cell. The FSS metallic cell is placed on the top of 5880 Rogers's substrate with 2.2, and 0.5 mm dielectric constant and thickness respectively and there is no metal sheet added on the other side of the substrate. The FSS cell is composed of two metallic rings connected to a rectangular strip with a thickness of 0.035 mm as illustrated in Fig. 9 (a). The FSS unit cell has a size of 5 mm × 5mm. A boundary condition of the unit cell as shown in Fig. 9 (b) is employed in the CST software to simulate the FSS cell and to accelerate the simulation process. For excitation, the Floquet ports in the ±z directions are utilized. Fig. 10 illustrates the S-parameters outcomes of the unit FSS cell. It is noticed that the FSS has band stop behavior with $S_{21} \leq -10$ dB extended from 26 GHz to 30 GHz and the deepest level of the S_{21} (-40 dB) is introduced at 28 GHz. As well, from Fig. 10, the S_{11} is very high in the band stop area so, the incoming EM waves are returned from the FSS-based reflectors at the frequency band around the operating frequency and the FSS is operated in this case as a reflector. Also, Fig. 10 shows the equivalent circuit
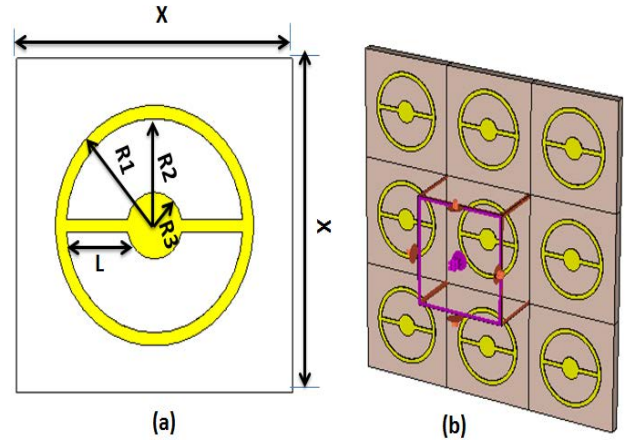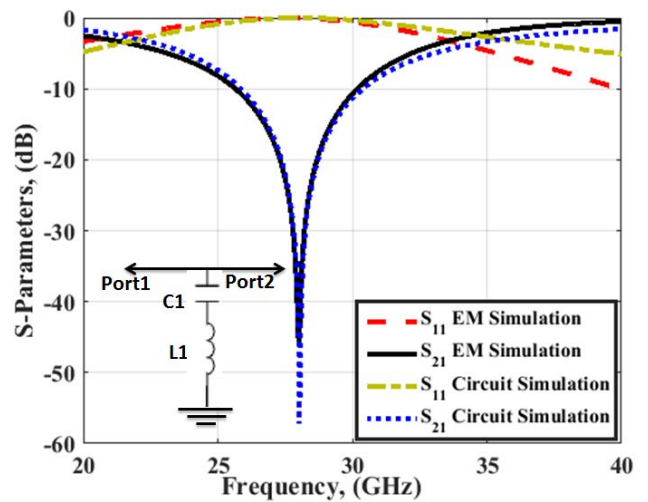

FIGURE 10. S-parameters outcomes of the proposed FSS unit cell.

model of the FSS cell. The equivalent circuit is composed of a series inductance with (L = 0.293 nH) and capacitor with (C = 0.11 pF) [30]. The comparison between the two S-parameters extracted from CST and circuit simulators is shown in Fig. 10 with a good matching between the two outcomes. To study the insensitivity to the polarization of the suggested FSS design, the direction of the propagation path of the EM waves is fixed, while the propagation path of the electric and magnetic fields are rotating with different polarization angles (φ) under normal incidence as shown in Fig. 11 (a). The polarization angles (φ) vary from 0º to 90º. It can be observed from Fig. 11(a) that the suggested FSS design gives the same performance for different polarization angles (φ). As well, for oblique angles of incident $\ominus$, the response of the FSS design is stable for angles up to 15^0 and shifted from the centered frequency for angles more than 15º as shown in Fig. 11 (b). For more analysis of the FSS cell, relative complex parameters such as permittivity and permeability have been discussed [31]. The FSS cell
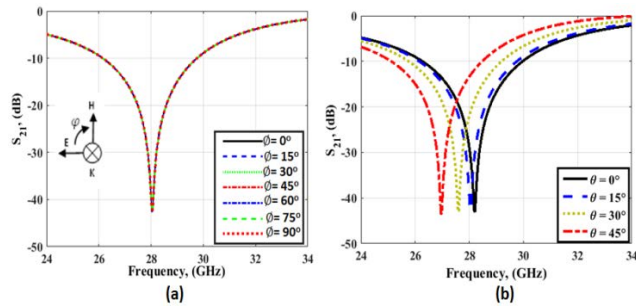
FIGURE 11. S_{21} results of the FSS cell with variation in (a) polarization angles (φ) under normal incidence (b) angle of incidence $\ominus$.
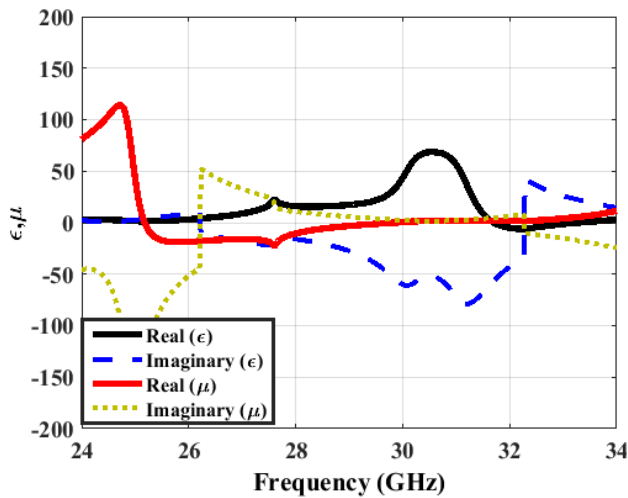

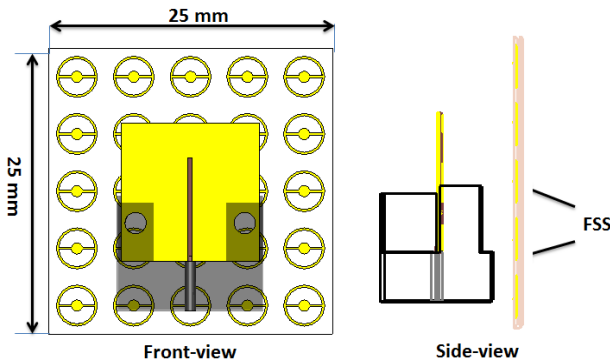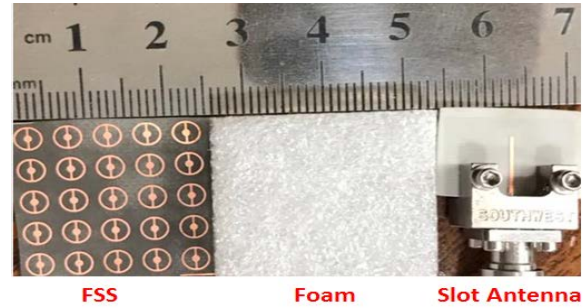**FIGURE 12.** FSS cell permittivity and permeability parameters.

FIGURE 13. Perspective view of the suggested antenna attached with the FSS.

FIGURE 14. Suggested fabricated antenna prototype photo attached with the 5 × 5 FSS based reflectors.
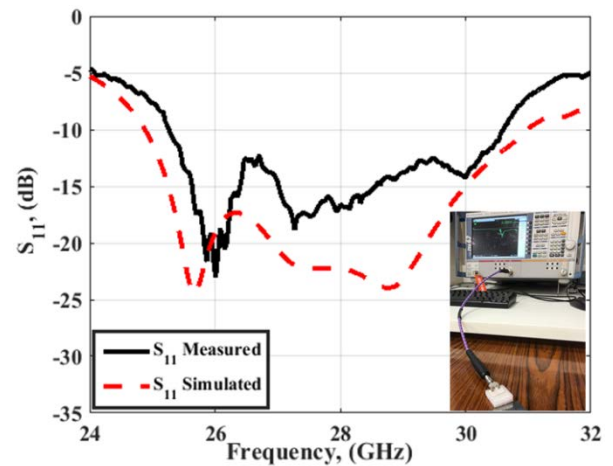
FIGURE 15. S_{11} outcomes of the suggested antenna attached with FSS.
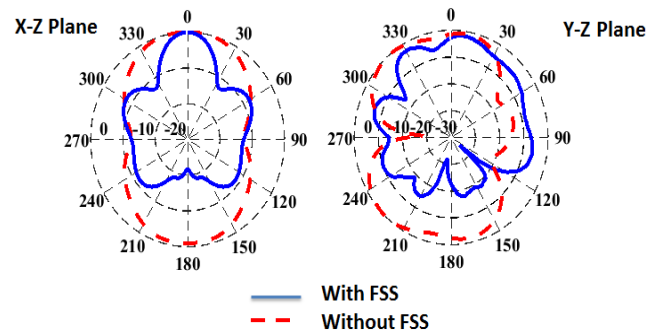
FIGURE 16. Radiation patterns simulation (normalized) with/without FSS at 28 GHz.

parameters can be extracted from S_{11} and S_{21} [31]. It can be seen from Fig. 12 that the relative parameters of the proposed FSS give a negative value at the resonant frequency and entire the frequency band which claim that the FSS cell can be considered a metamaterial structure.

IV. SLOT ANTENNA WITH FSS SIMULATION RESULTS AND DISCUSSION

To enhance the antenna gain, the suggested antenna is introduced in this section. The slot antenna is embedded with the designed FSS-based reflectors discussed previously. The

spacing between the antenna and the FSS-based reflectors also the FSS-based reflector's cell size is optimized to produce the desired antenna gain, S_{11}, and radiation efficiency
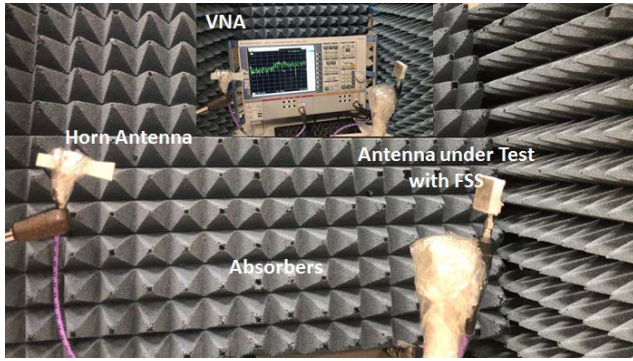
FIGURE 17. Radiation patterns and gain measuring setup of the antenna attached with FSS.
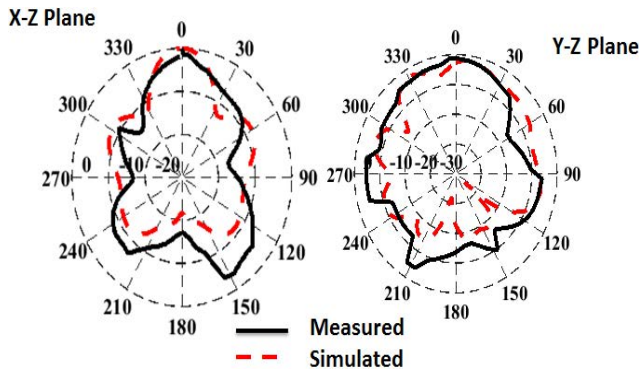
FIGURE 18. Normalized radiation patterns of the suggested slot antenna attached with FSS at 28 GHz.
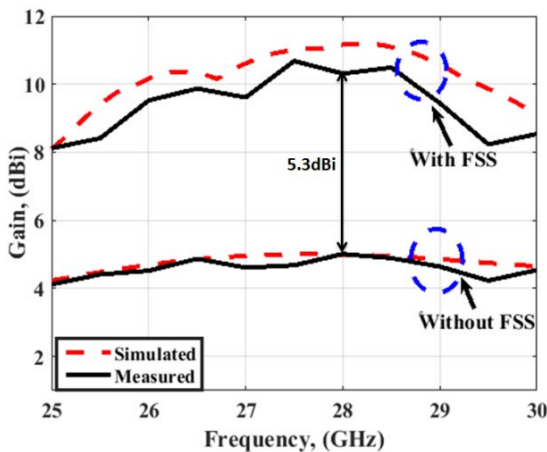
FIGURE 19. Suggested slot antenna attached with FSS realized gain.

features. The front and side views of the suggested antenna are shown in Fig. 13. A 5 × 5 FSS-based reflector is utilized and added under the slot antenna with an optimized separation of around 5 mm between them. The fabricated photo prototypes of FSS and slot antenna are illustrated in Fig. 14. To separate between the antenna and the FSS-based reflectors, a polystyrene layer (foam) with 1.03 and 5 mm dielectric constant and thickness is utilized as displayed in

FIGURE 20. Slot antenna attached with FSS efficiency.

Fig. 14. The same VNA is used in the measurement process and the tested outcomes in comparison with the simulated one are shown in Fig. 15.
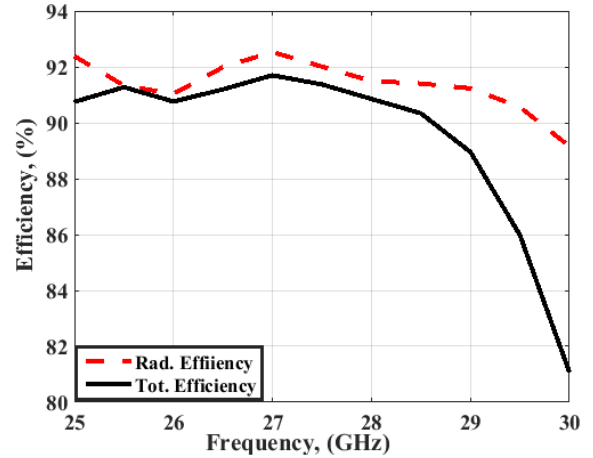
The simulated results have a frequency band with $S_{11} \leq -10$ dB from 25.2 GHz to 31 GHz (5.8 GHz bandwidth) and the measured outcomes achieved a frequency band from 25.5 GHz to 30.8 GHz (5.3 GHz bandwidth). The two outcomes have a good trend between them with small differences because of fabrication tolerance, FSS alignment, and some human errors in the fabrication process which can't be tackled. The simulated normalized radiation patterns with and without FSS at 28 GHz to show the effect of using FSS on the antenna performance are shown in Fig. 16. It is obvious that the FSS can improve the antenna radiation pattern, reduce the back loops of the single antenna without FSS and increase the antenna gain.

The gain and radiation pattern measuring setup of the suggested antenna with FSS is illustrated in Fig. 17. The same procedures discussed in the previous section are used to extract the radiation pattern and antenna gain. The normalized simulated and tested radiation patterns outcomes at 28 GHz in X-Z and Y-Z planes are displayed in Fig. 18. The antenna has unidirectional patterns in both planes with broad-side direction and with a good trend between the two outcomes. As well, the realized gain of the antenna is tested, and shown in Fig. 19. The simulated realized gain equals 11 dBi and around 10.3 dBi is achieved from the tested results at 28 GHz. The antenna has achieved a realized gain around 5.3dBi higher than the antenna without FSS-based reflectors as shown in Fig. 19. Fig. 20 illustrates the total and radiation efficiency of the suggested antenna. The efficiency of the antenna equals around 90.5 %. The reduction of the efficiency of the slot antenna is due to the presence of the new dielectric substrate and conductors of the FSS-based reflectors.

Table 1 illustrates the suggested work in comparison with other antenna designs. The suggested antenna has reasonable values of gain, bandwidth, efficiency, and miniaturizing size.

TABLE 1. Suggested work in comparison with other antenna designs.

Ref.		Antenna Size (mm^3)	εr / thickness (mm)	F_0/BW (GHz)	Number of elements	Technique used for gain enhancement	Gain (dBi)	Radiation Efficiency (%)
This work	Single	12 × 12 × 0.203	3.55/0.203	28/3.8	1	NA	4.5	93
	FSS	25 × 25 × 5	2.2/0.5	28/5.3	1	FSS	10.3	90
[13]		14.5 × 10 × 0.203	3.55/0.203	28/3.8	1	NA	5.8	NA
[14]		15 × 15× 0.203	3.55/0.203	28/6.3	1	NA	4.5	83
[15]		26.5 × 18.5 × 0.508	2.2/0.508	28/2.4	4	Array	10.3	83
[16]		30 × 19 × 1.6	4.3/1.6	28/3.6	5	Array	10.0	92
[17]		40 × 40 × 5.5	2.2/0.508	28/5.0	4	Array	12.5	92
[18]		45× 45× 0.254	2.2/0.254	32.5/11.5	8	Array	12.5	NA
[19]		30×16 × 0.8	2.2/0.8	33/7.0	1	AMC	5.5	66.5
[20]		47 × 47× 0.208	3.55/0.203	28/5.0	2	AMC	10.0	91
[21]		12.8 × 12.8× 0.5	3.66/0.5	28/5.7.0	1	AMC	7.8	80
[25]		32× 32 × 6.35	2.2/0.787	28/2.5	1	FSS	17.7	90
[26]		27.8 × 10.2 × 3.5	3.38/0.5	28/3.0	1	FSS	7.8	NA

Finally, from achieved frequency bands, antenna gain, and efficiency, it can be concluded that the suggested antenna can be recommended to be utilized in the new 5G NR application for n257 and n261standereds.

V. CONCLUSION

A slot antenna for new 5G networks with gain improvement has been presented. The FSS with 5 × 5 cells has been employed to achieve the required gain improvement. The suggested antenna has an overall dimension of 25 × 25 × 5 mm^3. The antenna without FSS-based reflectors has achieved bandwidth with $S_{11} \leq$ -10 dB and realized gain from 26 GHz to 29.8 GHz and around 4.5 dBi respectively. Whilst the antenna embedded with FSS has been achieved bandwidth with $S_{11} \leq$ -10 dB and realized gain from 25.5 GHz to 30.8 GHz and around 10.3dBi. A good tendency between the measured and simulated outcomes has been accomplished which supports the suggested antenna to be employed in the new 5G networks.

REFERENCES

[1] M. Abirami, "A review of patch antenna design for 5G," in *Proc. IEEE Int. Conf. Electr., Instrum. Commun. Eng. (ICEICE)*, Apr. 2017, pp. 1–3.

[2] J. Zhang, X. Yu, and K. B. Letaief, "Hybrid beamforming for 5G and beyond millimeter-wave systems: A holistic view," *IEEE Open J. Commun. Soc.*, vol. 1, pp. 77–91, 2020.

[3] Q. Yang, S. Gao, Q. Luo, L. Wen, Y.-L. Ban, X. Ren, J. Wu, X. Yang, and Y. Liu, "Millimeter-wave dual-polarized differentially fed 2-D multibeam patch antenna array," *IEEE Trans. Antennas Propag.*, vol. 68, no. 10, pp. 7007–7016, Oct. 2020.

[4] S.-J. Park, D.-H. Shin, and S.-O. Park, "Low side-lobe substrate-integrated-waveguide antenna array using broadband unequal feeding network for millimeter-wave handset device," *IEEE Trans. Antennas Propag.*, vol. 64, no. 3, pp. 923–932, Mar. 2016.

[5] M. Abdullah, S. H. Kiani, and A. Iqbal, "Eight element multiple-input multiple-output (MIMO) antenna for 5G mobile applications," *IEEE Access*, vol. 7, pp. 134488–134495, 2019.

[6] A. R. Sabek, W. E. Ali, and A. A. Ibrahim, "Minimally coupled two-element MIMO antenna with dual band (28/38 GHz) for 5G wireless communications," *J. Infr., Millim., THz Waves*, vol. 43, pp. 335–348, May 2022.

[7] S. H. Kiani, A. Altaf, M. Abdullah, F. Muhammad, N. Shoaib, M. R. Anjum, R. Damaševičius, and T. Blažauskas, "Eight element side edged framed MIMO antenna array for future 5G smart phones," *Micromachines*, vol. 11, no. 11, p. 956, 2020.

[8] S. Y. A. Fatah, E. K. I. K. I. Hamad, W. Swelam, A. M. M. A. Allam, M. F. A. Sree, and H. A. Mohamed, "Design and implementation of UWB slot-loaded printed antenna for microwave and millimeter wave applications," *IEEE Access*, vol. 9, pp. 29555–29564, 2021.

[9] Q. Zhu, K. Bo Ng, C. Hou Chan, and K.-M. Luk, "Substrate-integrated-waveguide-fed array antenna covering 57–71 GHz band for 5G applications," *IEEE Trans. Antennas Propag.*, vol. 65, no. 12, pp. 6298–6306, Dec. 2017.

[10] R. Przesmycki, M. Bugaj, and L. Nowosielski, "Broadband microstrip antenna for 5G wireless systems operating at 28 GHz," *Electronics*, vol. 10, no. 1, p. 1, Dec. 2020.

[11] G. Kim and S. Kim, "Design and Analysis of dual polarized broadband microstrip patch antenna for 5G mmWave antenna module on FR4 substrate," *IEEE Access*, vol. 9, pp. 64306–64316, 2021.

[12] A. Abdelaziz, H. A. Mohamed, and E. K. I. Hamad, "Applying characteristic mode analysis to systematically design of 5G logarithmic spiral MIMO patch antenna," *IEEE Access*, vol. 9, pp. 156566–156580, 2021.

[13] H. Zahra, W. A. Awan, W. A. E. Ali, N. Hussain, S. M. Abbas, and S. Mukhopadhyay, "A 28 GHz broadband helical inspired end-fire antenna and its MIMO configuration for 5G pattern diversity applications," *Electronics*, vol. 10, no. 4, p. 405, Feb. 2021.

[14] N. Hussain, W. A. Awan, W. Ali, S. I. Naqvi, A. Zaidi, and T. T. Le, "Compact wideband patch antenna and its MIMO configuration for 28 GHz applications," *AEU, Int. J. Electron. Commun.*, vol. 132, Apr. 2021, Art. no. 153612.

[15] M. M. Kamal, S. Yang, S. H. Kiani, D. A. Sehrai, M. Alibakhshikenari, M. Abdullah, F. Falcone, E. Limiti, and M. Munir, "A novel hook-shaped antenna operating at 28 GHz for future 5G mmWave applications," *Electronics*, vol. 10, no. 6, p. 673, Mar. 2021.

[16] J. A. Nasir, M. U. Rehman, A. J. Hashmi, and W. T. Khan, "A compact low cost high isolation substrate integrated waveguide fed slot antenna array at 28 GHz employing beamforming and beam scanning for 5G applications," in *Proc. 12th EuCAP*, London, U.K., 2018, p. 5.

[17] O. M. Haraz, A. Elboushi, S. A. Alshebeili, and A.-R. Sebak, "Dense dielectric patch array antenna with improved radiation characteristics using EBG ground structure and dielectric superstrate for future 5G cellular networks," *IEEE Access*, vol. 2, pp. 909–913, 2014.

[18] S. X. Ta, H. Choo, and I. Park, "Broadband printed-dipole antenna and its arrays for 5G applications," *IEEE Antennas Wireless Propag. Lett.*, vol. 16, pp. 2183–2186, 2017.

[19] A. A. Althuwayb, "MTM-and SIW-inspired bowtie antenna loaded with AMC for 5G mm-wave applications," *Int. J. Antennas Propag.*, vol. 2021, Jan. 2021, Art. no. 6658819.

[20] A. A. Ibrahim and W. A. E. Ali, "High gain, wideband and low mutual coupling AMC-based millimeter wave MIMO antenna for 5G NR networks," *AEU, Int. J. Electron. Commun.*, vol. 142, Dec. 2021, Art. no. 153990.

[21] W. Wan, M. Xue, L. Cao, T. Ye, and Q. Wang, "Wideband low-profile AMC-based patch antenna for 5G antenna-in-package application," in *Proc. IEEE 70th Electron. Compon. Technol. Conf. (ECTC)*, Jun. 2020, pp. 1818–1823.

[22] A. Hocini, N. Melouki, and T. A. Denidni, "Modeling and simulation of an antenna with optimized AMC reflecting layer for gain and front-to-back ratio enhancement for 5G applications," *J. Phys., Conf. Ser.*, vol. 1492, no. 1, Apr. 2020, Art. no. 012006.

[23] A. J. A. Al-Gburi, I. B. M. Ibrahim, M. Y. Zeain, and Z. Zakaria, "Compact size and high gain of CPW-fed UWB strawberry artistic shaped printed monopole antennas using FSS single layer reflector," *IEEE Access*, vol. 8, pp. 92697–92707, 2020.

[24] A. Chatterjee and S. K. Parui, "Frequency-dependent directive radiation of monopole-dielectric resonator antenna using a conformal frequency selective surface," *IEEE Trans. Antennas Propag.*, vol. 65, no. 5, pp. 2233–2239, May 2017.

[25] M. Asaadi, I. Afifi, and A.-R. Sebak, "High gain and wideband high dense dielectric patch antenna using FSS superstrate for millimeter-wave applications," *IEEE Access*, vol. 6, pp. 38243–38250, 2018.

[26] M. Mantash, A. Kesavan, and T. A. Denidni, "Beam-tilting endfire antenna using a single-layer FSS for 5G communication networks," *IEEE Antennas Wireless Propag. Lett.*, vol. 17, no. 1, pp. 29–33, Jan. 2018.

[27] U. Nissanov, G. Singh, and N. Kumar, "High gain microstrip array antenna with SIW and FSS for beyond 5G at THz band," *Optik*, vol. 236, Jun. 2021, Art. no. 166568.

[28] M. A. E.-A. Abo-Elhassan, A. E. Farahat, and K. F. A. Hussein, "Millimetric-wave quad-band MIMO antennas for future generations of mobile communications," *Prog. Electromagn. Res. B*, vol. 95, pp. 41–60, 2022.

[29] A. E. Farahat and K. F. A. Hussein, "Dual-band (28/38 GHz) wideband MIMO antenna for 5G mobile applications," *IEEE Access*, vol. 10, pp. 32213–32223, 2022.

[30] A. R. Varkani, Z. H. Firouzeh, and A. Z. Nezhad, "Equivalent circuit model for array of circular loop FSS structures at oblique angles of incidence," *IET Microw., Antennas Propag.*, vol. 12, no. 5, pp. 749–755, Apr. 2018.

[31] M. Edries, H. A. Mohamed, S. S. Hekal, M. A. El-Morsy, and H. A. Mansour, "A new compact quad-band metamaterial absorber using interlaced I/square resonators: Design, fabrication, and characterization," *IEEE Access*, vol. 8, pp. 143723–143733, 2020.

HESHAM A. MOHAMED (Senior Member, IEEE) received the B.Sc. degree in electronics and communication engineering from the University of Menofia, in 2003, and the M.Sc. and Ph.D. degrees from Ain Shams University, in 2009 and 2014, respectively. He has teaching experience (more than 12 years' experience) as a Lecturer at the Electronic and Communication Engineering Department, Faculty of Engineering, Misr University for Science and Technology. He is currently an Associate Professor with the Electronics Research Institute (ERI), Giza, Egypt. He has authored or coauthored close to 30 journal articles, about 17 refereed conference papers, and attend and chaired several national and international conferences. He has supervised and co-supervised four Ph.D. and four M.Sc. theses at Cairo University, Ain Shams University, Benha University, and Helwan University. He has the outstanding publications of his work in ranked international journals and conferences. He participates in more than six research projects at the national and international levels as Egypt-NSF-USA Joint Fund Program, Egypt STDF-France IRD Joint Fund Program, and the European Committee Programs of FP6 and FP7. His role is from a C-PI to a PI. As a RF-Design Engineer of antenna and power amplifier module, he was (2018–2020) in the Project "Small SAR Satellite Antenna and Transceiver System" and communication subsystem engineering (2019–2020) in the Project "Egyptian University Satellite (EUS-2)." As a RF-Design Engineer, he was (2018–2019) in the Project "Design of Radar Absorbing Materials (RAM) Using Meta-Materials" wireless system engineering and in the Project (2015–2018) "Development of High Data Rate X-Band Transmitter for LEO Remote Sensing Satellites." As a RF-Design Engineer, he was (2015–2018) in the Project "THE EGYPTIAN 2D RADAR." As a RF-Design Engineer, he was (2011–2014) in the Project "Ultra-Wideband Ground Penetrating Radar for Water Detection, Egypt." As a RF-Design Engineer, he was (February 2011–February 2014) in the Project "Novel Planar Antennas for the Most Recent Telecommunications Applications." His research interests include microwave circuit designs, planar antenna systems, recently on EBG structures, UWB components and antenna and RFID systems, radar absorbing materials, energy harvesting and wireless power transfer, smart antennas, microstrip antennas, microwave filters, metamaterials, and MIMO antennas and its applications in wireless communications. He is a Reviewer at the international journal as following, IEEE MICROWAVE AND WIRELESS COMPONENTS LETTERS, IEEE ACCESS, *Progress in Electromagnetics Research* (PIER), *PIER B*, *PIER C*, *PIER M*, *PIER Letters*, *Microwave and Optical Technology Letters*, and the *International Journal of Circuit Theory and Applications*.

MOHAMED EDRIES received the B.Sc. degree in electronics and communication engineering from the Higher Institute of Engineering, El Shorouk, Cairo, Egypt, in 2007, the M.Sc. degree in electronics and communication engineering from Al Azhar University, Cairo, in 2016, and the Ph.D. degree in electronics and communication engineering from Benha University, Cairo, in 2020. He currently works with the Higher Institute of Engineering. His research interests include antenna and RFID systems, radar absorbing materials, energy harvesting and wireless power transfer, smart antennas, microstrip antennas, microwave filters, metamaterials, wireless and optical communications, optical CDMA, and digital design with VHDL.

MAHMOUD A. ABDELGHANY (Member, IEEE) received the B.Sc. degree in electrical engineering and the M.Sc. degree in communication engineering from Minia University, in 2000 and 2005, respectively, and the Ph.D. degree from Kyushu University, Japan, in 2011. In December 2011, he joined the Electrical Engineering Department, Faculty of Engineering, Minia University, as an Assistant Professor. He has worked as a Postdoctoral Research Fellow at the Radio-Frequency Integrated Circuits (RFIC) and Microwave Communication Devices Laboratory, Kyushu University, from October 2013 to April 2014. Since January 2018, he has been an Assistant Professor with the College of Engineering, Prince Sattam Bin Abdulaziz University, Saudi Arabia. His current research interests include the study and design of RF CMOS System LSI, and low-power, low-noise, and highly linear CMOS RF front-end architectures.

AHMED A. IBRAHIM (Senior Member, IEEE) was born in 1986. He received the B.Sc., M.Sc., and Ph.D. degrees in electrical engineering from the Electronic and Communication Engineering Department, Minia University, Minya, Egypt, in 2007, 2011, and 2014, respectively. He has been a Visiting Professor with University Pierre and Marie Curie, Sorbonne Université, Paris VI, France, for seven months; and Otto-von-Guericke-Universität Magdeburg, Germany, for six months. He is currently an Associate Professor with the Electrical Engineering Department, Faculty of Engineering, Minia University. He has published more than 95 peer-reviewed journals and conference papers. His research interests include miniaturized multiband antennas/wideband, microwave/millimeter components, DRA metamaterial antenna, graphene antenna, and microwave filters. His research interests also include MIMO antennas and energy harvesting systems. He is a Senior Member of URSI and a member of the National Committee of Radio Science in Egypt. From 2020 to 2021, he was named in the top 2% of scientists in "A standardized citation metrics author database annotated for scientific field" and "Updated science-wide author databases of standardized citation indicators." He is a Reviewer in IEEE ANTENNAS AND WIRELESS PROPAGATION LETTERS, IEEE MICROWAVE AND WIRELESS COMPONENTS LETTERS, IEEE ACCESS, *IET Microwaves, Antennas and Propagation*, *Electronics Letters* (IET), *MOTL*, *Analog Integrated Circuits and Signal Processing*, and many other journals and conferences.

● ● ●